

# Influence of Magnetic Field and Temperature on the Transient Density and Voltage in a Radial Junction Solar Cell in Dynamic Regime under Pulsed Multispectral Illumination

Moussa Ouedraogo<sup>1</sup>, Nazé Yacouba Traore<sup>1</sup>, Alain Diasso<sup>2</sup>, Raguilignaba Sam<sup>1,2</sup>, François Zougmore<sup>2</sup>

<sup>1</sup>Laboratoire de Matériaux, d'Héliophysique et Environnement (LaMHE), Département de Physique, UFR/ST Université Nazi Boni, Bobo Dioulasso, Burkina Faso

<sup>2</sup>Laboratoire de Matériaux et Environnement, Département de Physique, UFR/SEA, Université Joseph Ki-Zerbo, Ouagadougou, Burkina Faso

Email: mouedraogosh@gmail.com

**How to cite this paper:** Ouedraogo, M., Traore, N.Y., Diasso, A., Sam, R. and Zougmore, F. (2025) Influence of Magnetic Field and Temperature on the Transient Density and Voltage in a Radial Junction Solar Cell in Dynamic Regime under Pulsed Multispectral Illumination. *Open Journal of Applied Sciences*, 15, 42-52.

<https://doi.org/10.4236/ojapps.2025.151004>

**Received:** November 19, 2024

**Accepted:** January 13, 2025

**Published:** January 16, 2025

Copyright © 2025 by author(s) and Scientific Research Publishing Inc. This work is licensed under the Creative Commons Attribution International License (CC BY 4.0).

<http://creativecommons.org/licenses/by/4.0/>



Open Access

## Abstract

This study examines the influence of magnetic field and temperature on the transient voltage of a polycrystalline silicon radial junction solar cell in a dynamic regime under multispectral illumination. Radial junction solar cells represent a major advancement in photovoltaic technologies, as they optimize light absorption and charge collection efficiency. The focus is on the impact of the magnetic field and temperature on the decay of transient voltage, which provides crucial information on recombination processes and the lifetime of minority carriers. The results reveal that the magnetic field tends to increase the transient voltage by directly affecting the transient electron density. Indeed, for  $B > 7 \times 10^{-5}$  T, the magnetic field prolongs the relaxation time by increasing the transient voltage amplitude. Additionally, rising temperatures accelerate (ranging from 290 K to 450 K) recombination processes, thereby reducing the transient voltage, although this effect is moderated by the presence of a magnetic field. The study highlights the complex interaction between magnetic field and temperature, with significant impacts on the transient behaviour.

## Keywords

Electrons, Radial Junction, Transient Voltage, Magnetic Field, Operating Temperature

## 1. Introduction

This Radial junction solar cells represent a major advancement in photovoltaic technologies by optimizing light absorption [1] [2]. They utilize structures such as silicon nanowires (SiNW), vertically aligned micro-wires, and conical micro-wires to improve light collection and charge collection efficiency [3] [4]. These strategies, including high-purity doping processes, enhance light absorption and reduce surface reflection, thereby improving the overall efficiency of radial junction solar cells [4] [5]. Compared to traditional planar cells, radial cells offer superior efficiency by optimizing the management of photons and charge carriers. Compatible with various semiconductor materials and adaptable to flexible devices, they significantly contribute to the transition towards sustainable renewable energy. Innovative nanowire designs can achieve energy conversion efficiencies of up to 17.57%, surpassing traditional texturing models [6].

In parallel, the transient voltage of a solar cell is crucial for analyzing recombination processes and minority carrier lifetimes, which are essential for optimizing cell performance [7]. It manifests during the transition between two stable operating states, such as when the cell is suddenly switched to an open-circuit condition after optical or electrical excitation. This transient response, influenced by charge variations, electromagnetic interference [8], and operating temperature, is characterized by its duration, amplitude, and shape before stabilizing. It provides valuable information on recombination parameters and helps determine the effective lifetime of minority carriers [8] [9]. While transient voltage has been extensively studied for bifacial cells [8]-[10], its analysis in the context of polycrystalline silicon radial junction solar cells remains limited. Therefore, this study aims to develop an analytical expression for the transient voltage of radial cells and to examine the impact of magnetic fields and temperature on their transient.

## 2. Theory

### 2.1. Modeling of the Radial Junction Solar Cell

Radial junction solar cells represent an alternative geometry compared to traditional planar solar cells, with remarkable electrical and optical performance. This study focuses on a radial junction solar cell based on polycrystalline silicon. The polycrystalline substrate is composed of very small cylindrical grains, which are separated by transition zones known as grain boundaries. These grain boundaries act as recombination centers, thus influencing both the macroscopic and microscopic parameters of the cell.

The model of the studied cell is illustrated in **Figure 1** below.

The cell has a cylindrical shape with a radius  $R$  and a depth  $H$ , segmented into four distinct regions:

- An N-doped region, characterized by a width  $e_1$ , where free electrons are the majority carriers and holes are the minority carriers.
- A P-doped region, with a width  $b_1$ , where free holes are the majority carriers and electrons are the minority carriers.

- An intermediate region, with a width ranging between  $[b_2, e_2]$ , forms at the interface between the N and P regions, where a concentration gradient of electrons and holes emerges across the contact surface. When contact is established between the N and P zones, free charge carriers (electrons and holes) diffuse from the region where they are in excess to the region where they are deficient. In the P region, the depleted zone becomes negatively charged due to the presence of negative acceptor ions, while in the N region, it becomes positively charged due to positive donor ions. This region, composed of fixed charges, is referred to as the Space Charge Region (SCR) or depletion zone.

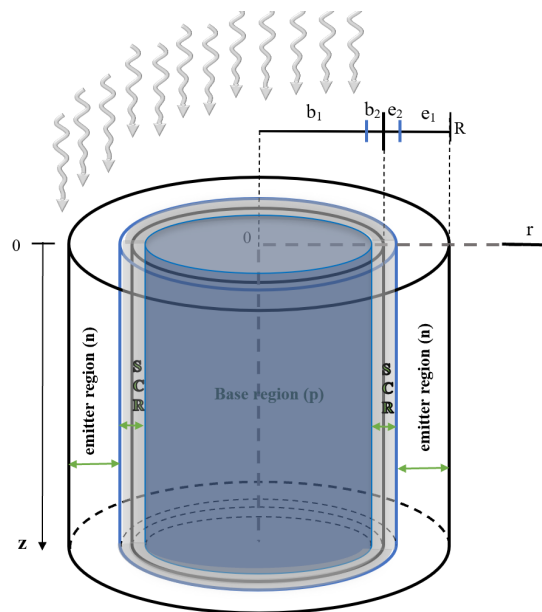


**Figure 1.** Model of a radial junction photovoltaic cell.

The formation of the PN junction generates an electric field  $\vec{E}$  (diffusion field) directed from the N side (positively charged) to the P side (negatively charged), associated with a potential known as the diffusion potential or barrier potential  $V_b$ . This internal field opposes the diffusion of electrons and holes, leading to a state of equilibrium.

Under illumination, the electron-hole pairs generated by light are separated by this electric field. The electrons are drawn toward the N-doped region, while the holes migrate toward the P-doped region, resulting in the generation of a photocurrent [11]. Illumination increases this reverse current by generating electron-hole pairs not only in the SCR but also in the doped regions. This PN junction forms the core of the photovoltaic cell, enabling it to function as an electrical generator under illumination.

## 2.2. Continuity Equations of Charge Carriers

The continuity equation for the excess photogenerated minority charge carriers in the base and emitter regions is given by:

$$\frac{\partial^2 \delta(r, z, t)}{\partial r^2} + \frac{1}{r} \frac{\partial \delta(r, z, t)}{\partial r} + \theta^2 \frac{\partial^2 \delta(r, z, t)}{\partial z^2} - \frac{\delta(r, z, t)}{L_n^{*2}} + \frac{g(z)}{D^*} = \frac{1}{D^*} \frac{\partial \delta(r, z, t)}{\partial t} \quad (1)$$

where:

$L^*$  and  $D^*$  designate the respective length and diffusion coefficient of charge carriers under the influence of magnetic fields and temperature.

In the formulation of these equations, the magnetic field is oriented along the depth  $z$ :  $\vec{B} = B \cdot \vec{z}$ .

$\delta = \delta_n$  represents the excess electron density generated in the base region, while  $\delta = \delta_p$  represents the excess hole density generated in the emitter region.  $g(z)$  is the generation rate of photogenerated electron-hole pairs, which depends on the cell's penetration depth. For multispectral illumination, it is expressed by Equation (2), and the coefficients  $a_i$  and  $b_i$  are determined based on the AM 1.5 solar irradiance [12].

$$g(z) = \begin{cases} \sum_{i=1}^4 a_i \cdot \exp(-b_i z) & \text{Si } 0 \leq z \leq T_e \\ 0 & \text{Si } z > T_e \end{cases} \quad (2)$$

The boundary conditions that the cell adheres to are as follows: [12]-[14]:

At the center of the solar cell ( $r = 0$ )

$$\delta_n(r = 0, z, t) = \text{finie} \quad (3)$$

- At the junction ( $r = b_1$ )

$$\delta_n(r = b_1, z, t) = n_o \left( \exp\left(\frac{V}{V_t}\right) - 1 \right) \quad (4)$$

- At the front face of the cell ( $z = 0$ )

$$\delta_n(r, z = 0, t) = 0 \quad (5)$$

- the rear side ( $z = H$ )

$$\left. \frac{\delta_n(r, z, t)}{\partial z} \right|_{z=H} = -\frac{S_b}{D_n^*} \delta_n(r, z = H, t) \quad (6)$$

To solve the continuity Equation (1) in the base region, we employ superposition in the following form [15]:

$$\delta_n(r, z, t) = \psi_n(r, z, t) + \phi_n(r) \quad (7)$$

$\phi_n(r)$  represents the non-homogeneous form of the partial differential equation (PDE), describing its steady state with the generation term. Its solution is given by Equation (8).

$$\phi(r) = \left[ n_o \left( \exp\left(\frac{V}{V_t}\right) - 1 \right) - \frac{L_n^{*2}}{D_n^*} g(z) \right] \frac{I_0(L_n^{*-1} \cdot r)}{I_0(L_n^{*-1} \cdot r_b)} + \frac{L_n^{*2}}{D_n^*} g(z) \quad (8)$$

where  $I_0$  is the modified Bessel function of the first kind of order 0. The transient formulation of the homogeneous form  $\psi_n(r, z, t)$  of the PDE has the solution:

$$\psi_n(r, z, t) = \sum_{k=0}^{\infty} \sum_{m=0}^{\infty} C_{km} \cdot J_o(\beta_{n,m} \cdot r) \cdot \cos(\sigma_{n,k} \cdot z) \times \exp(-D_n^* \cdot \lambda_{n,km}^2 (t - T_e)) \quad (9)$$

With  $C_{n,km}$ , a constant that we determined when the cell is in steady state

$$C_{k,m} = \frac{\int_{z=0}^H \int_{r=0}^{b_1} r \Delta n(r, z) J_o(\beta_{n,m} \cdot r) \cos(\sigma_{n,k} \cdot z) dr \cdot dz}{\int_{r=0}^{b_1} r \cdot J_o^2(\beta_{n,m} \cdot r) dr \times \int_{z=0}^H \cos^2(\sigma_{n,k} \cdot z) dz} \quad (10)$$

With  $\Delta n(r, z)$  the electron density in steady-state determined through the same assumptions.

The parameters  $\sigma_{n,k}$ ,  $\beta_{n,m}$ ,  $\lambda_{n,km}$  and  $w_{ww}$  are eigenvalues determined from the previously mentioned boundary conditions. The transient voltage represents the temporal variation of the voltage generated by the cell between two stable operating states. It can be measured at the terminals of a solar cell, initially excited by a light flux or an electric voltage, and then suddenly placed in an open-circuit condition [8]-[10]. This voltage is related to the concentration of charge carriers at the junction. According to the Boltzmann relation, its expression is given by:

$$V_{\alpha}(t) = V_T \cdot \ln\left(1 + r_{\alpha} \cdot F(H, b_2) \exp(-D_n^* \cdot \lambda_{km}^2 (t - T_e))\right) \quad (11)$$

$t \leq T_e$  corresponds to the excitation phase of the cell.  $t > T_e$  corresponds to the decay of the carrier density after the excitation signal is interrupted. The transient voltage is obtained during the phase where  $t > T_e$ .

$F(H, b_1)$  is called the reduced amplitude of the transient voltage (Diasso thesis). Its value depends on the grain size, recombination velocities at the interfaces, the intensity of the magnetic field, and the operating temperature of the cell. Its expression is given by:

$$F(H, b_1) = \sum_{k=0}^{\infty} \sum_{m=0}^{\infty} \frac{\frac{C_{km} \cdot \theta_n}{\sigma_k} J_o(\beta_m \cdot b_1) \sin\left(\frac{\sigma_k \cdot H}{\theta_n}\right)}{K_{n,i} I_o(\beta_{n,i} b_1) \sin\left(\frac{\sigma_{n,i} H}{\theta_n}\right) + n_o \left(\exp\left(\frac{V}{V_t}\right) - 1\right) H} \quad (12)$$

Expression (11) allows for predicting two types of transient voltage behaviour.

- When  $t$  approaches  $t_0$ , that is, near the point 0 which defines the voltage  $V_0$ , the transient voltage given by expression (11) takes the following approximate form:

$$V_{\alpha}(t) = V_T \cdot \left[-D_n^* \cdot \lambda_{km}^2 (t - T_e) + \ln(r_{\alpha} \cdot F(H, b_1))\right] \quad (13)$$

Transient voltage is a linear function of time.

- When  $t$  approaches infinity, that is, far from the point 0 and in the vicinity of the point defining the voltage  $V_0$ , the transient voltage approximates the following form:

$$V_{\alpha}(t) = V_T \cdot r_{\alpha} \cdot F(L, b_1) \exp(-D_n^* \cdot \lambda_{km}^2 (t - T_e)) \quad (14)$$

In this case, the transient voltage is an exponentially decreasing function of time.

### 3. Results and Discussion

#### 3.1. Effects of the Magnetic Field on the Transient Electron Density

During normal operation of a solar cell, electron-hole pairs are continuously generated by light radiation. When the light source is abruptly turned off (at  $t = T_e$ ), this generation stops, and the excess electrons recombine or diffuse, gradually reducing their density. This rapid decrease in electron density, as observed in **Figure 2**, then converges towards a new stationary equilibrium where recombination and diffusion balance out.

We analyze the influence of the magnetic field on the transient electron density in the base through the profiles shown in **Figure 2** below:

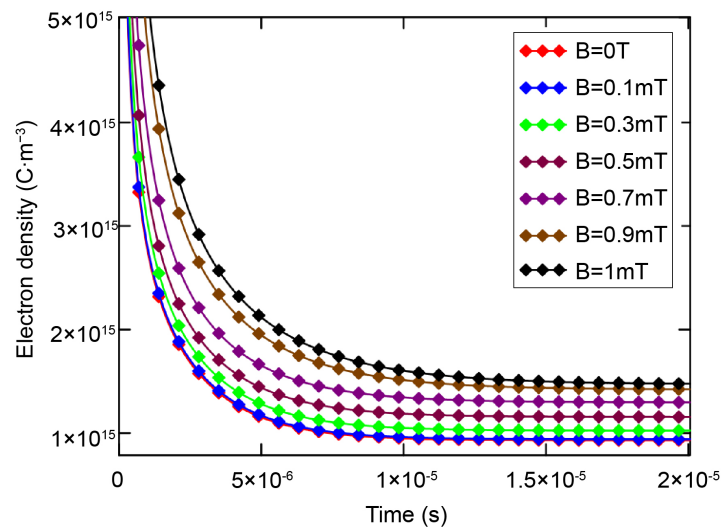


**Figure 2.** Variation of electron density over time for several values of the magnetic field:  $b_1 = 300 \mu\text{m}$ ,  $H = 300 \mu\text{m}$ ,  $B = 0.1 \text{ mT}$ .

These results show that under the influence of weak magnetic fields ( $B = 0$  to  $0.1 \text{ mT}$ ), the electron density in the solar cell decreases rapidly, allowing for a faster return to a new equilibrium state. In contrast, with stronger magnetic fields (up to  $1 \text{ mT}$ ), this decrease is slower because the Lorentz force alters the trajectories of the electrons, reducing their mobility and slowing down their recombination. This phenomenon maintains a high electron density for a longer period, which could be advantageous in applications requiring prolonged charge carrier conservation [16], thereby improving the efficiency of the solar cell by extending energy storage after the light source is turned off.

#### 3.2. Effects of Temperature on the Transient Electron Density

**Figure 3** shows the effect of temperature on the transient density.

The curves show that the electron density decreases more slowly at higher temperatures. This can be explained by the fact that an increase in temperature results in higher thermal energy availability, which slows down electron recombination due

to their increased thermal agitation.

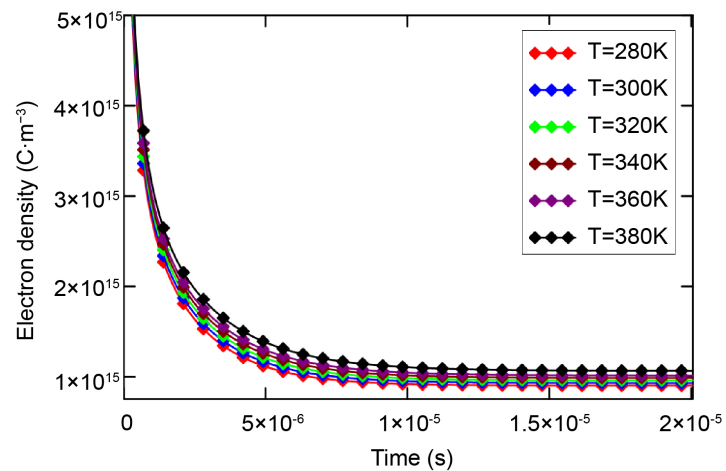


**Figure 3.** Variation of electron density over time for several values of temperature:  $b_1 = 300 \mu\text{m}$ ,  $H = 300 \mu\text{m}$ ,  $B = 0.1 \text{ mT}$ .

At lower temperatures, recombination occurs more rapidly, leading to a faster decrease in electron density. This means that the cell reaches a new steady-state equilibrium more quickly at lower temperatures.

After the initial transient phase, the electron density stabilizes at a new steady-state equilibrium. This equilibrium is characterized by a balance between recombination and diffusion processes.

The curves also show that this equilibrium is reached at higher electron densities when the temperature is higher. This may indicate that even after the light source is turned off, the cell retains a higher concentration of residual charge carriers at elevated temperatures. This could potentially impact the solar cell's efficiency, particularly under operating conditions where the base temperature is high. It is crucial to consider this thermal effect when designing and optimizing solar cells for optimal performance.

### 3.3. Effects of the Magnetic Field on the Transient Voltage

In **Figure 4**, we present the decay curves of the transient voltage as a function of time with different values of the magnetic field.

The obtained profiles show that the transient voltage decreases exponentially over time, quickly tending toward zero, regardless of the magnetic field value. However, for low magnetic field values ( $B < 7 \times 10^{-5} \text{ T}$ ), the amplitude of the transient voltage remains almost unchanged (**Figure 3**), indicating that low magnetic fields do not significantly influence the charge carrier density.

In this case, the transient voltage decreases more rapidly. Conversely, once the magnetic field exceeds  $7 \times 10^{-5} \text{ T}$ , an increase in the amplitude of the transient voltage is observed, along with a slower decrease. This suggests that the magnetic field affects the relaxation time of the transient voltage. Indeed, the increase in the

magnetic field seems to slow down the recombination of charge carriers, resulting in a more gradual decrease in the transient voltage. This could be due to the Lorentz force, which alters the movement of charge carriers (electrons and holes) in the solar cell, reducing their recombination rate while causing their accumulation at the junction.

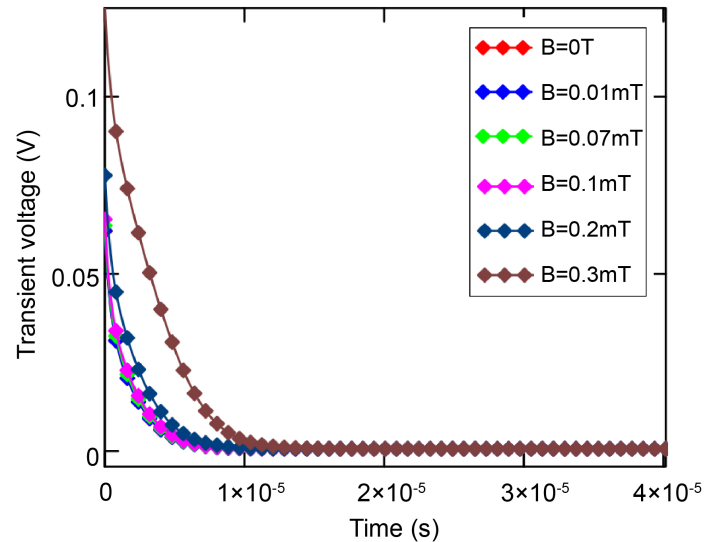


**Figure 4.** Transient voltage profile as a function of time for various magnetic field values  $b_1 = 300 \mu\text{m}$ ,  $H = 300 \mu\text{m}$ ;  $T = 300\text{K}$ .

After a certain time ( $\sim 15 \times 10^{-5}$  s), all curves converge to a zero voltage, indicating that the system reaches its equilibrium state regardless of the applied magnetic field.

### 3.4. Effects of Temperature on the Transient Voltage

**Figure 5(a)** and **Figure 5(b)** respectively illustrate the variations in transient voltage profiles over time for different temperatures, both in the absence of a magnetic field and in the presence of a significant magnetic field.

In **Figure 5(a)**, where  $B = 0$  T, the transient voltage decreases rapidly over time for all the temperatures studied. It is observed that temperature has a minimal effect on the initial amplitude and the rate of decline of the transient voltage. The curves are very similar, indicating that, without a magnetic field, temperature does not significantly influence the transient behaviour of the solar cell.

In contrast, in **Figure 5(b)**, where  $B = 0.2$  mT, although the transient voltage also decreases rapidly over time, more pronounced differences appear depending on the temperature. Under the influence of the magnetic field, the effect of temperature becomes more pronounced. Specifically, at higher temperatures (for example,  $T = 450$  K), the initial amplitude of the transient voltage is lower, and the decline is faster compared to lower temperatures. This suggests that the magnetic field amplifies the effect of temperature on the charge carrier dynamics in the solar cell.

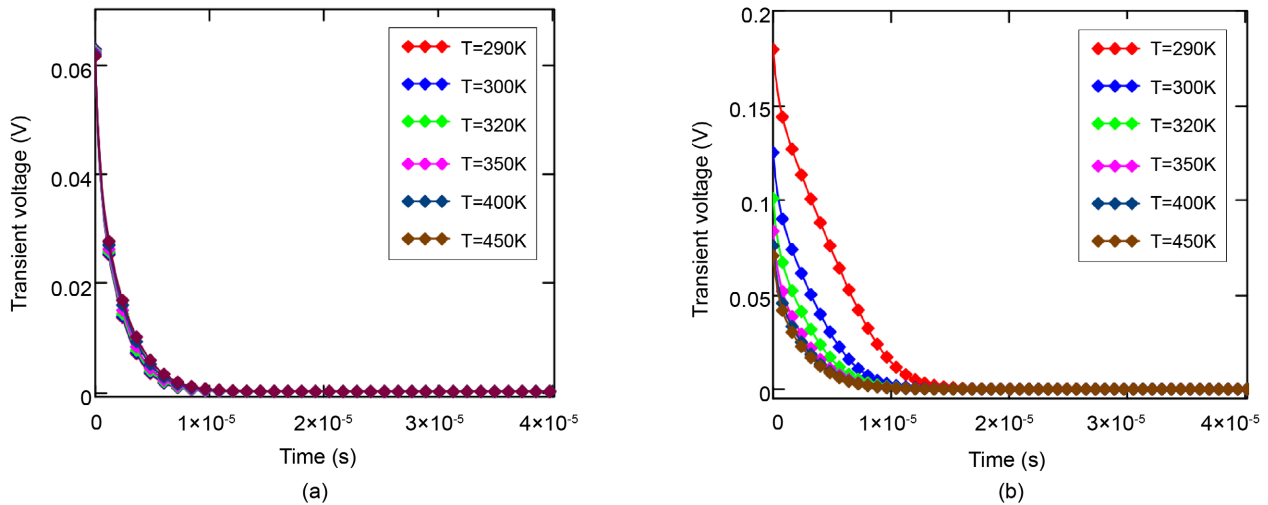


**Figure 5.** (a) Effect of temperature on transient voltage in the absence of a magnetic field ( $B = 0$  T); (b) Effect of temperature on transient voltage in the presence of a magnetic field ( $B = 0.2$  mT):  $b_1 = 300$   $\mu\text{m}$ ,  $H = 300$   $\mu\text{m}$ .

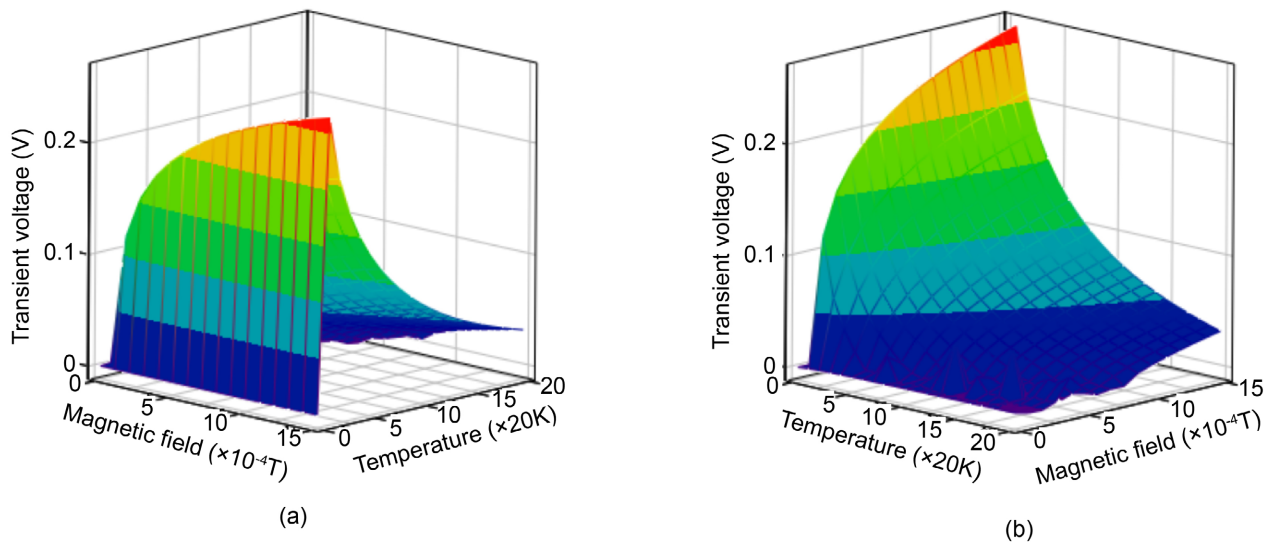


**Figure 6.** Combined effect of temperature and magnetic field on transient voltage  $b_1 = 300$   $\mu\text{m}$ ,  $H = 300$   $\mu\text{m}$ .

To better appreciate the combined effect of the magnetic field and temperature on the transient voltage, we created a 3D representation of these two effects, as shown in the two curves of **Figure 6**.

These curves show that the transient voltage initially increases with the rise in the magnetic field, reaching a peak before decreasing (curve 6.a). This behaviour indicates that the magnetic field strongly influences the dynamics of charge carriers, especially at lower temperatures. As the temperature increases, the influence of the magnetic field on the transient voltage appears to diminish, which may be due to the acceleration of charge carrier recombination processes.

In curve 6.b, it is observed that the transient voltage varies depending on both temperature and the magnetic field, reaching maximum values for specific combinations of these two parameters. At higher temperatures, the transient voltage

is lower for all levels of the magnetic field, confirming the combined effect of the magnetic field and temperature on the transient behaviour of the solar cell.

These 3D visualizations clearly show that the transient voltage in the radial junction solar cell is strongly influenced by the interaction between the magnetic field and temperature, with more complex and significant effects when these two parameters are considered together.

#### 4. Conclusion

Through this study, we have demonstrated that the transient voltage in a radial junction solar cell is strongly influenced by the interaction between the magnetic field and temperature. The magnetic field, by altering the trajectories of charge carriers, slows down their recombination, resulting in an increase in the transient voltage. Conversely, an increase in temperature accelerates carrier recombination, thereby reducing the lifetime of minority carriers and consequently decreasing the transient voltage. When these two parameters are considered together, their effects become more complex and significant, highlighting the importance of a joint analysis to optimize the performance of radial junction solar cells. These findings provide avenues for improving the design and efficiency of solar cells, particularly through the precise determination of certain optoelectronic parameters such as carrier lifetime.

#### Conflicts of Interest

The authors declare no conflicts of interest regarding the publication of this paper.

#### References

- [1] Ali, N.M., Allam, N.K., Abdel Haleem, A.M. and Rafat, N.H. (2014) Analytical Modeling of the Radial PN Junction Nanowire Solar Cells. *Journal of Applied Physics*, **116**, Article ID: 024308. <https://doi.org/10.1063/1.4886596>
- [2] Raj, V., Zhu, Y., Vora, K., Fu, L., Tan, H.H. and Jagadish, C. (2023) Pushing Limits of Photovoltaics and Photodetection Using Radial Junction Nanowire Devices. 2022 *IEEE International Conference on Emerging Electronics (ICEE)*, Bangalore, 11-14 December 2022, 1-7.
- [3] Zhang, S., Wang, S., Hu, R., Cao, Y., Wang, J., Xu, J., *et al.* (2023) How Backreflection Contributes to Light Absorption for High-Performance Radial Junction Photovoltaics. *Applied Physics Letters*, **123**, Article ID: 231102. <https://doi.org/10.1063/5.0174700>
- [4] Vismara, R., Isabella, O., Ingenito, A., Si, F.T. and Zeman, M. (2019) Geometrical Optimisation of Core-Shell Nanowire Arrays for Enhanced Absorption in Thin Crystalline Silicon Heterojunction Solar Cells. *Beilstein Journal of Nanotechnology*, **10**, 322-331. <https://doi.org/10.3762/bjnano.10.31>
- [5] Raj, V., Fu, L., Tan, H.H. and Jagadish, C. (2019) Design Principles for Fabrication of INP-Based Radial Junction Nanowire Solar Cells Using an Electron Selective Contact. *IEEE Journal of Photovoltaics*, **9**, 980-991. <https://doi.org/10.1109/jphotov.2019.2911157>
- [6] Cabrera-España, F.J. and Rahman, B.M.A. (2023) Optical and Electrical Analyses of

- Solar Cells with a Radial PN Junction and Incorporating an Innovative NW Design That Mimics ARC Layers. *Nanomaterials*, **13**, Article 1649. <https://doi.org/10.3390/nano13101649>
- [7] Chibane, Y., Kouhlane, Y., Bouhafs, D. and Zerguine, A. (2023) Light Induced Degradation Quantification by Monitoring the VOC Output of Silicon Solar Cell Using Low-Cost Real-Time Virtual Instrumentation. *Journal of Sustainable Materials Processing and Management*, **3**, 28-38. <https://doi.org/10.30880/jsmpm.2023.03.02.003>
- [8] Barro, F.I., Maiga, A.S., Wereme, A. and Sissoko, G. (2010) Determination of Recombination Parameters in the Base of a Bifacial Silicon Solar Cell under Constant Multispectral Light. *Physical and Chemical News*, **56**, 76-84.
- [9] Sam, R., Zouma, B., Zougmore, F., Koalaga, Z., Zoungrana, M. and Zerbo, I. (2012) 3D Determination of the Minority Carrier Lifetime and the P-N Junction Recombination Velocity of a Polycrystalline Silicon Solar Cell. *IOP Conference Series: Materials Science and Engineering*, **29**, Article ID: 012018. <https://doi.org/10.1088/1757-899x/29/1/012018>
- [10] Diasso, A., Sam, R., Zouma, B. and Zougmore, F. (2020) Experimental Measurement of Minority Carriers Effective Lifetime in Silicon Solar Cell Using Open Circuit Voltage Decay under Magnetic Field in Transient Mode. *Smart Grid and Renewable Energy*, **11**, 181-190. <https://doi.org/10.4236/sgre.2020.1111011>
- [11] Mohammadi, V., Nihtianov, S. and Fang, C. (2021) Author Correction: A Doping-Less Junction-Formation Mechanism between N-Silicon and an Atomically Thin Boron Layer. *Scientific Reports*, **11**, Article No. 20579. <https://doi.org/10.1038/s41598-021-99821-9>
- [12] Trabelsi, A., Zouari, A. and Arab, A.B. (2009) Modeling of Polycrystalline N+/P Junction Solar Cell with Columnar Cylindrical Grain. *Revue des Energies Renouvelables*, **12**, 279-297.
- [13] Kayes, B.M., Atwater, H.A. and Lewis, N.S. (2005) Comparison of the Device Physics Principles of Planar and Radial P-N Junction Nanorod Solar Cells. *Journal of Applied Physics*, **97**, Article ID: 114302. <https://doi.org/10.1063/1.1901835>
- [14] Leye, S.N., Fall, I., Mbodji, S., Sow, P.L.T. and Sissoko, G. (2018) Analysis of T-Coefficients Using the Columnar Cylindrical Orientation of Solar Cell Grain. *Smart Grid and Renewable Energy*, **9**, 43-56. <https://doi.org/10.4236/sgre.2018.93004>
- [15] Hahn, D.W. and NecatiOzisik, M. (2012) Heat Conduction. Third Edition, Wiley.
- [16] Verma, M. and Gautam, S. (2023) Photovoltaic Efficiency Enhancement via Magnetism. *Journal of Magnetism and Magnetic Materials*, **588**, Article ID: 171436. <https://doi.org/10.1016/j.jmmm.2023.171436>